Available online at www.sciencedirect.com

ScienceDirect

Ceramics International 40 (2014) 1687–1692

CERAMICS INTERNATIONAL

www.elsevier.com/locate/ceramint

Microstructure evolution and optical properties of *c*-axis-oriented ZnO thin films incorporated with silver nanoisland layers

Yuan-Chang Liang*, Xian-Shi Deng

Institute of Materials Engineering, National Taiwan Ocean University, Keelung 20224, Taiwan

Received 19 June 2013; received in revised form 11 July 2013; accepted 11 July 2013
Available online 20 July 2013

Abstract

Highly *c*-axis-oriented ZnO thin films incorporated with various numbers of Ag nanoisland layers were fabricated in this study by alternating sputtering-deposited ZnO and Ag layers on Si substrates. Two such ZnO–Ag layered structures were fabricated: the first by using a 150-nm ZnO film–Ag island layer/Si, and the second by using three applications of a 50-nm ZnO film–Ag island layer/Si. The crystallographic features of the as-deposited ZnO thin film on the Si substrate exhibited a pure *c*-axis orientation. However, the degree of the *c*-axis texture of the ZnO thin films slightly decreased after inserting Ag island layers. The ZnO thin-film surface became quite rough because the surface morphology was transformed from being dense and flat to exhibit a loosely columnar grain structure. Transmittance electron microscopy (TEM) images showed that the Ag islands were clearly distributed on the ZnO/substrate and ZnO/ZnO interfaces. The photoluminescence measurement results indicated that the near-band-edge (NBE) emission peak intensity was enhanced by nearly two orders of magnitude in the 150-nm ZnO film–Ag island layer/Si compared with that of the as-deposited 150-nm ZnO thin film without an inserted Ag island layer. Inserting additional Ag island layers did not increase the NBE emission intensity; instead, the visible emission band intensity was markedly increased. This was attributed to the substantial change in the ZnO thin film microstructure caused by inserting the Ag island layers.

Keywords: A. Films; B. Defects; B. Surfaces; C. Optical properties

1. Introduction

ZnO is a promising semiconductor for various optoelectronic and optical applications because of the following properties: a wide band gap and a high exciton binding energy (60 meV) at room temperature [1]. The excellent thin-film structure of ZnO is essential for practical device applications.

Although various physical and chemical methodologies have been proposed to prepare ZnO thin films that demonstrate desired electrical and optical properties [2–5], vacuum thin-film processes, such as sputtering, are considered the most favorable deposition methods for obtaining highly uniform films because they enable precise control of thickness, actualize large-area deposition, facilitate the doping process, and produce multilayer structures [6–8]. Sputtering is widely used in processing semiconductor devices. This vacuum thin film process realizes the integration of ZnO thin-film processes into Si-based devices. Recently, a ZnO-based multilayer structure containing an ultrathin metal film was proposed to broaden the optical and electrical properties of ZnO for device applications [6]. These ZnO-based multilayer structures have been used as transparent conducting electrodes or optical fibers in various optoelectronic devices [9]. Several ZnO-based multilayer systems, such as ZnO/Ru/ZnO, ZnO/Cu/ZnO, ZnO/Al/ZnO, and ZnO/Ag/ZnO, have been fabricated using vacuum processes, and their optical absorption, transmittance, and electrical properties have been investigated [6,10,11].

By controlling the relative thickness of ZnO and metals, regulating the number of layers in a multilayer structure, and choosing a proper metal as an interlayer, improving the intrinsic electrical and optical properties of ZnO in ZnO-metal composite structures is possible. Recently, substantial photoluminescence (PL) enhancement of ZnO films was

*Corresponding author.
E-mail address: yuanvictory@gmail.com.

0272-8842/$ - see front matter © 2013 Elsevier Ltd and Techna Group S.r.l. All rights reserved.
http://dx.doi.org/10.1016/j.ceramint.2013.07.060

achieved by coating metal nanoparticles on ZnO surfaces through surface plasmon coupling [12]. Surface plasmons excited on thin metallic structures/dielectric interfaces have been used to enhance the luminescence of light-emitting materials and devices [12,13]. Among various plasmonic metal materials, it has been shown that Ag particles have strong interactions with visible light through the resonance of the oscillations of the electrons within them. Although a ZnO–Ag–ZnO multilayer system is promising for use in transparent contact electrodes because of its low resistivity and satisfactory optical transmittance property, reports on the correlation between the microstructure and PL properties of the layered ZnO–Ag thin-film structures are still limited. In this study, various layered structures consisting of ZnO film and Ag nanoislands were fabricated by using sputtering to investigate the microstructure-dependent PL properties. This will expand the application of ZnO-metal layered structures in optical and optoelectronic devices.

2. Experimental

ZnO–Ag single and multilayer thin films were sputter deposited on silicon substrates using ZnO and Ag targets. The substrates were supersonic clean out in acetone, rinsed in alcohol and subsequently dried in flowing air gas before deposition. The ultra-thin Ag film was deposited at 20 mTorr under an Ar atmosphere at room temperature and the Ag sputtering duration was 25 s. The Ag island film on the Si substrate can be obtained after annealing at 300 °C in vacuum for 1 h. The ZnO layer was subsequently deposited onto the Ag island film to form single ZnO–Ag layer thin film. The multilayer ZnO–Ag structure was also prepared by alternating deposition of Ag and ZnO layers. The working pressure for ZnO thin film growth is fixed at 30 mTorr with a pure Ar atmosphere. A fixed total thickness of 150 nm for ZnO was designed for all single and multilayer films.

X-ray diffraction (XRD) with Cu Ka radiation was used to investigate the crystalline quality of the prepared thin films. The surface morphology was investigated with a field emission scanning electron microscopy (FESEM). The detailed structure of the ZnO–Ag thin films was further characterized by high-resolution transmission electron microscopy (HRTEM). The composition analysis is performed using EDS attached to the TEM. The room temperature dependent photoluminescence (PL) spectra are obtained using the 325 nm line of a He–Cd laser.

3. Results and discussion

The insets of Fig. 1 display the ZnO–Ag thin-film configuration. The ZnO single-layer film was also grown for comparison. Fig. 1 shows the XRD patterns of the ZnO, single-ZnO–Ag-layer, and multi-ZnO–Ag-layer thin films. Fig. 1(a) shows a strong Bragg reflection by ZnO (002). The hexagonal ZnO structure has a *c*-axis lattice constant of approximately 0.52 nm calculated according to the (002) peak; no additional crystallographic planes were observed, revealing that the ZnO thin film was highly *c*-axis textured. By inserting

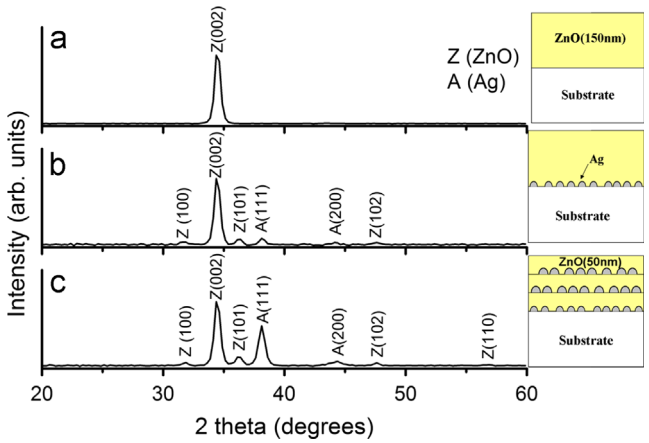

Fig. 1. XRD patterns of the ZnO thin films with and without Ag island layers: (a) without Ag island layer, (b) with one Ag island layer, and (c) with three Ag island layers. The configuration of the samples are shown in the insets.

an Ag island layer, clear Bragg reflections of (111) and (200) for the metallic Ag was observed for the single-ZnO–Ag-layer thin film. The peak intensity of Ag increased as more Ag was inserted for the triple-ZnO–Ag-layer thin film. Comparatively, a relatively strong peak intensity was observed for the (111) of the metallic Ag, revealing a preferred (111) growth of metallic Ag islands on the Si substrate and ZnO layer. No Bragg reflection from the oxidation phases of Ag was observed in this work, and pure metallic Ag-dielectric ZnO heterostructures were formed. In addition to strong Bragg reflections of ZnO (002), however, several crystallographic planes of ZnO (100), (101), (102), and (110) were observed, as shown in Fig. 1(b) and (c). This reveals that the Ag underlayer impairs the growth of *c*-axis-oriented ZnO crystals. The peak intensity ratios of (002) Bragg reflections to all crystallographic planes, $I(002)/[I(100)+I(002)+I(101)+I(102)+I(110)]$, in the polycrystalline ZnO thin films were calculated. Before the calculation, the background intensity of the Bragg reflections was initially deducted. The relative intensity ratios for the single-layer-ZnO–Ag and triple-layer-ZnO–Ag thin films were approximately 0.86 and 0.79, respectively. The triple-layer thin film exhibited a more random crystallographic orientation because the Ag islands might not have provided suitable crystallographic compatibility for the *c*-axis growth of ZnO.

Fig. 2(a)–(c) shows the surface morphology of ZnO, single-ZnO–Ag-layer, and triple-ZnO–Ag-layer thin films. The surface of the ZnO thin film without an Ag island underlayer is flat and dense, and no pores were observed on the surface. The size range of the ZnO thin-film surface grains was approximately 50–80 nm. Fig. 2 (b)–(c) illustrates how the surface of the ZnO-based thin films became rough by adding the Ag island underlayer. Regarding the single-ZnO–Ag-layer film, the surface grain size exhibited a large distribution, ranging from 50 to 150 nm. Moreover, regarding the triple-ZnO–Ag-layer thin film, the range was approximately 40–125 nm. The compactness of the film surface decreased as the number of ZnO–Ag layers increased. The triple-ZnO–Ag-layer thin film exhibited a columnar grain structure, and clear gaps among the

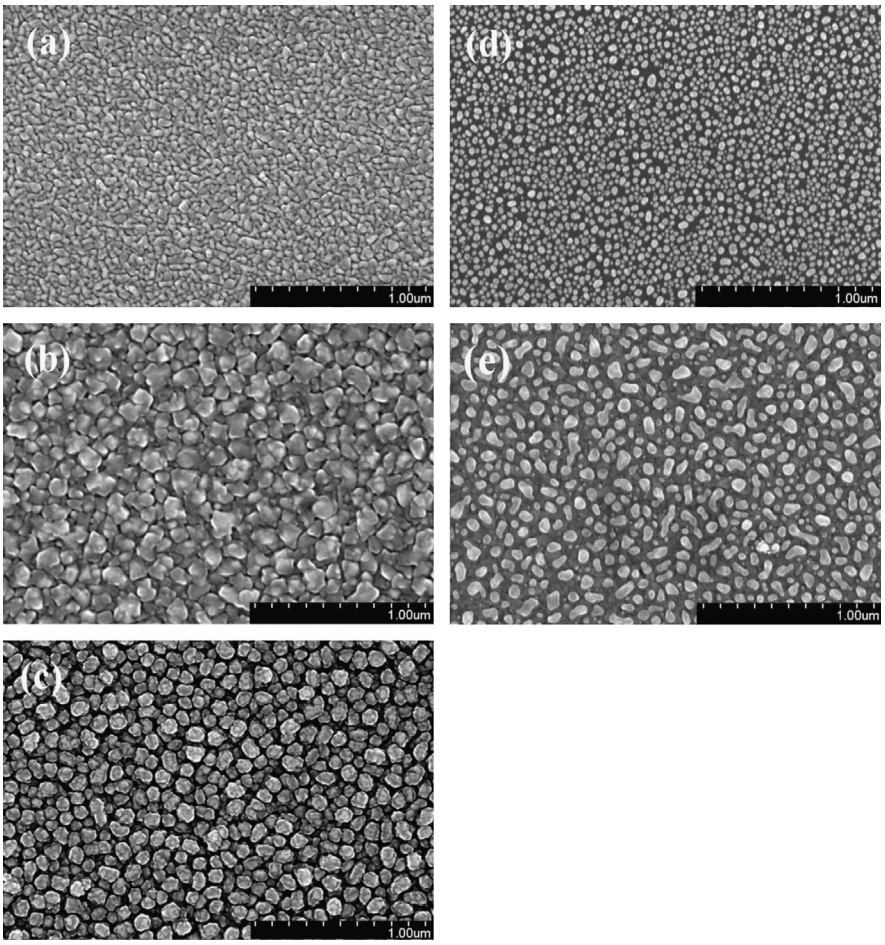

Fig. 2. SEM images of the ZnO thin films with and without Ag island layers: (a) without Ag island layer, (b) with one Ag island layer, (c) with three Ag island layers, (d) Ag island layer on the Si substrate, and (e) Ag island layer on the ZnO film.

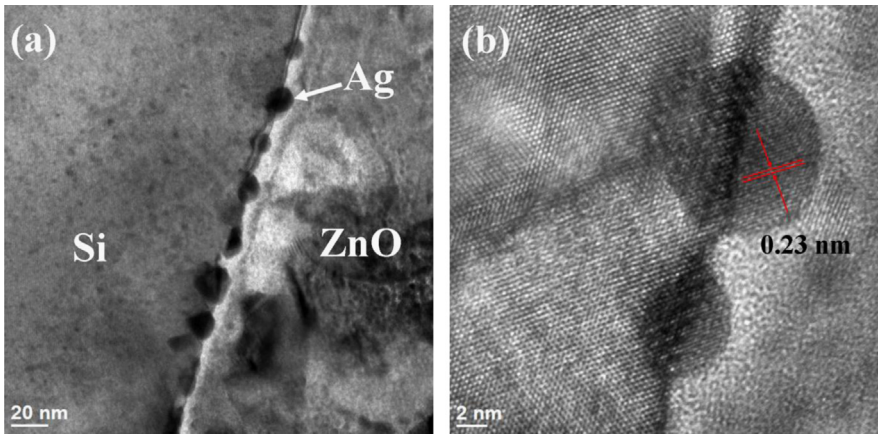

Fig. 3. (a) Cross-sectional TEM image of the 150 nm ZnO film–Ag island layer/Si, and (b) HRTEM image of (a).

grains were visible. Such a rugged surface morphology may indicate that crystal defects form more easily in multilayer film structures than in dense film structures. To understand more clearly the causes of the different surface morphologies of the single-ZnO–Ag-layer and triple-ZnO–Ag-layer thin films, the sizes of Ag islands on the Si substrate and ZnO thin film produced under the same sputtering duration and annealing conditions were further investigated. Notably, as seen in Fig. 2 (d)–(e), the Ag islands were homogeneously dispersed over the area of interest on the Si substrate. However, the distribution of Ag islands was relatively inhomogeneous on the ZnO thin film. The sizes of Ag islands on the Si substrate were relatively

smaller than that on the ZnO thin film; in addition, the shape of the Ag islands on the Si substrate was spherical, whereas on the ZnO thin film, it was irregular-shaped. These differences might account for the formation of separated columnar grains on the triple-ZnO–Ag-layer thin film.

Fig. 3(a) shows a low-magnification cross-sectional TEM image of the single-ZnO–Ag-layer thin film taken from the interface of Si and ZnO with an Ag nanoisland layer inserted at the interface. Ag nanoislands with a typical diameter of approximately 10–18 nm were attached to the Si substrate. The high-resolution transmission electron microscopy (HRTEM) image in Fig. 3(b) shows Ag nanoislands with clear lattice fringes that can be indexed to the (111) plane of metallic Ag. Fig. 4(a) shows a low-magnification cross-sectional TEM image of the triple-ZnO–Ag-layer thin film. A clear ZnO–Ag layered structure was formed on the substrate. The selected area electron diffraction (SAED) pattern taken from the ZnO–Ag-layered structure exhibited clear spots and a ring-like feature (Fig. 4(b)), and the corresponding crystallographic planes of the spots and ring patterns were indexed. The clear spots were identified as crystalline ZnO phases, whereas the ring patterns were ascribed to the formation of metallic Ag nanoislands in the ZnO. Fig. 4(c) shows the energy dispersive X-ray spectroscopy (EDS) line scan profiling crossing the sample. A clear compositional modulation of Zn and Ag signals was observed, showing the effectively ZnO–Ag-layered structure. Moreover, the elemental mapping of Zn and Ag shown in Fig. 4(d) indicates that the Ag nanoislands were distributed between the ZnO layers.

Fig. 5 shows the PL spectra of the various samples measured at room temperature. The control sample, which consisted of pure ZnO thin film on the Si substrate, shows a typical PL spectrum composed of a strong near-band edge (NBE) emission band at approximately 3.25 eV and a relatively weak yellow–green emission band at approximately 2.18 eV. This visible emission band was attributed in a previous study to oxygen vacancy in oxides [5]. In this work, the ZnO thin films were prepared in an oxygen-deficient environment; thus, oxygen vacancies were assumed to form easily during thin film preparation [14]. The ZnO thin film with a thin layer of Ag nanoislands distributed on the substrate showed a marked enhancement of UV emission band intensity without a noticeable increase in the visible emission band intensity. The UV peak intensity of the single-ZnO–Ag-layer thin film was increased by as much as double that of the ZnO thin film. The enhancement of UV emission was attributed to the resonant coupling between the localized surface plasmon resonance of the Ag nanoislands and NBE emission of the ZnO thin film. A similar UV emission enhancement mechanism was reported on the Ag nanoparticles decorated on ZnO nanorod arrays [15]. By contrast, the PL spectrum for the triple ZnO–Ag layer thin film showed no further enhancement of UV emission intensity. Instead, a marked increase in the visible emission band intensity was observed. A previous study showed that the size and shape of metal islands determine the resonance energy of a generated surface plasmon [16]. Furthermore, both larger metal particles and a higher

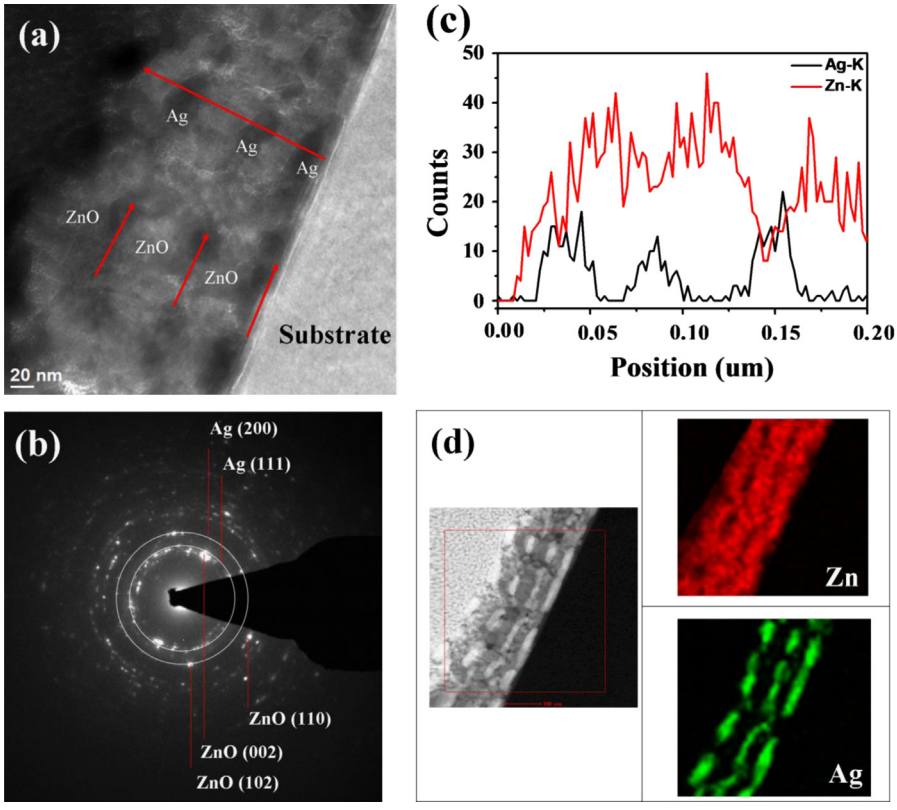

Fig. 4. (a) Cross-sectional TEM image of the (50 nm ZnO film–Ag island layer)$_3$/Si, (b) SEAD pattern of the ZnO–Ag multilayered thin film, (c) EDS line scan profiling taken along the red line as exhibited in (a), (d) Zn and Ag element mapping images taken from the red square region.

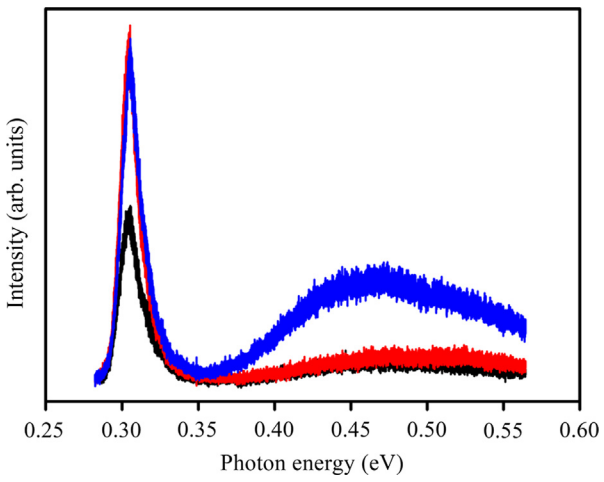

Fig. 5. PL spectra of the ZnO thin films with and without Ag island layers: black line: 150 nm ZnO film/Si, red line: 150 nm ZnO film–Ag island layer/Si, and blue line: triple-50 nm ZnO film–Ag island layer/Si. (For interpretation of the references to color in this figure legend, the reader is referred to the web version of this article.)

distribution density guarantee a stronger coupling of surface plasmons to light [17]. However, the Ag nanoislands in this work were formed by using a continuous ultra-thin Ag film with a fixed thickness after annealing. An increase in the Ag nanoisland size resulted in a decrease in the Ag nanoisland density. The multilayer ZnO–Ag structure herein caused a random distribution of the Ag nanoislands in the confined thin film structure; moreover, the size and density of the Ag nanoislands on the lowest layer (substrate surface) and middle layers (ZnO surfaces) were different (larger particle size and lower density on the ZnO surfaces). These factors might suppress the effectively resonant coupling between the localized surface plasmon resonance of Ag nanoislands and the NBE of ZnO films. A substantial increase of visible emission band intensity combined with a considerable decrease of UV emission band intensity was reported on ZnO nanorod arrays with an insertion of Ag island film between the substrate and rod-like ZnO film [16]. In this work, the enhancement of yellow–green emission band intensity did not accompany a noticeable decrease in UV emission band intensity. The mechanism of an increase of visible emission band intensity herein is not consistent with the previous report [16]. The microstructure changes in ZnO–Ag thin films, as caused by the number of Ag island layers, should be considered. Both crystallographic features and surface morphology account for the PL properties of the ZnO thin films. Based on the XRD results, an increase of Ag nanoisland layers slightly increases the formation ratio of non-polar crystals in the ZnO film. A previous study showed that native defects were energetically favorable and easier to form during the growth of non-polar ZnO than in the growth of polar ZnO. A well-suppressed value of the UV to the visible intensity ratio of ZnO rod-like film was observed with a marked increase in the non-polar crystal ratio [18]. Based on the SEM analysis results, the surface grains of the ZnO–Ag thin films changed from being a dense and flat surface to exhibiting a column-like surface with clearly apparent intervals. The loose surface microstructure of ZnO thin films might incur numerous crystal defects during thin film growth. The peak intensity of ZnO (002) Bragg reflections did not dramatically decrease by increasing the number of ZnO–Ag layers from one to three, and only the relative intensity ratio of (002) to all crystallographic planes was slightly decreased from 0.86 to 0.79. Therefore, the intensity of the UV emission band was not markedly changed. However, the marked increase of visible emission band intensity for the triple-ZnO–Ag-layer thin film might be associated with the slightly changed crystallographic features and the largely changed surface morphology of ZnO thin films because of the insertion of the Ag nanoisland layers. A discernible decrease in the UV-to-visible-intensity ratio of PL has been demonstrated in the electrochemically deposited ZnO thin film because the morphology of the ZnO thin film transformed from a dense and flat film surface to a loose rod-like film-surface structure [5].

4. Conclusions

ZnO-Ag-layered thin films were grown on the Si substrates by alternating sputtering-deposited ZnO and Ag layers. The XRD results showed that the as-deposited ZnO thin film without an inserted Ag island layer was *c*-axis textured. The insertion of Ag island layers in the ZnO thin films caused the microstructural changes. The highly *c*-axis-oriented crystallographic features of the ZnO thin film were slightly decreased, and the surface of the ZnO thin film became quite rough. TEM images showed that the Ag nanoislands were clearly distributed on the ZnO/substrate and ZnO/ZnO interfaces. Comparatively, the PL results showed that the NBE emission peak intensity was enhanced by nearly two orders of magnitude for the 150-nm ZnO–Ag island layer/Si composited thin film. This was attributed to the plasmon resonances of Ag nanoislands with the light. However, inserting additional Ag nanoisland layers in the ZnO thin film caused the different sizes and distribution densities of the Ag nanoislands on the Si substrate and ZnO surfaces. These changes suppressed the effectively resonant coupling between the localized surface plasmon resonances with light and did not increase the NBE emission intensity further. Instead, the visible emission band intensity was markedly increased because the ZnO thin-film microstructure deteriorated after inserting the Ag nanoisland layers.

Acknowledgments

This work is supported by the National Science Council of Taiwan (Grant nos. NSC102-2221-E-019-006-MY3, NSC100-2628-E-019-003-MY2 and NSC100-2221-E-019–059-MY2) and National Taiwan Ocean University (Grant no. NTOU-RD-AA-2012–104012).

References

[1] K. Vijayalakshmi, K. Karthick, P. Dhivya, M. Sridharan, Low power deposition of high quality hexagonal ZnO film grown on Al_2O_3 (0001) sapphire by dc sputtering, Ceramics International 39 (2013) 5681–5687.

[2] P. Prepelita, R. Medianu, B. Sbarcea, F. Garoi, M. Filipescu, The influence of using different substrates on the structural and optical characteristics of ZnO thin films, Applied Surface Science 256 (2010) 1807–1811.

[3] C.Y. Zhang, X.M. Li, X. Zhang, W.D. Yu, J.L. Zhao, Seed-layer induced growth of high-quality oriented ZnO films by a sol–gel process, Journal of Crystal Growth 290 (2006) 67–72.

[4] D. Podobinski, S. Zanin, A. Pruna, D. Pullini, Effect of annealing and room temperature sputtering power on optoelectronic properties of pure and Al-doped ZnO thin films, Ceramics International 39 (2013) 1021–1027.

[5] Y.C. Liang, M.Y. Tsai, C.L. Huang, C.Y. Hu, C.S. Hwang, Structural and optical properties of electrodeposited ZnO thin films on conductive RuO_2 oxides, Journal of Alloys and Compounds 509 (2011) 3559–3565.

[6] Y.C. Liang, X.S. Deng, H. Zhong, Structural and optoelectronic properties of transparent conductive *c*-axis-oriented ZnO based multilayer thin films with Ru interlayer, Ceramics International 38 (2012) 2261–2267.

[7] L. Balakrishnan, S. Gowrishankar, N. Gopalakrishnan, Fabrication of tridoped *p*-ZnO thin film and homojunction by RF magnetron sputtering, Ceramics International 38 (2012) 6221–6227.

[8] Y.C. Liang, Growth and characterization of nonpolar *a*-plane ZnO films onperovskite oxides with thin homointerlayer, Journal of Alloys and Compounds 508 (2010) 158–161.

[9] S.H. Mohamed, Effects of Ag layer and ZnO top layer thicknesses on the physical properties of ZnO/Ag/Zno multilayer system, Journal of Physics and Chemistry of Solids 69 (2008) 2378–2384.

[10] D.R. Sahu, J.L. Huang, Dependence of film thickness on the electrical and optical properties of ZnO–Cu–ZnO multilayers, Applied Surface Science 253 (2006) 915–918.

[11] M.F. Al-Kuhaili, M.A. Al-Maghrabi, S.M.A. Durrani, I.A. Bakhtiari, Investigation of ZnO/Al/ZnO multilayers as transparent conducting coatings, Journal of Physics D: Applied Physics 41 (2008) 215302–215310.

[12] W.H. Ni, J. An, C.W. Lai, H.C. Ong, J.B. Xu, Emission enhancement from metallodielectric-capped ZnO films, Journal of Applied Physics 100 (2006) 026103–026106.

[13] K. Okamoto, I. Niki, A. Shvartser, Y. Narukawa, T. Mukai, A. Scherer, Surface-plasmon-enhanced light emitters based on InGaN quantum wells, Nature Materials 3 (2004) 601–605.

[14] Y.C. Liang, H.Y. Lee, Growth of epitaxial zirconium-doped indium oxide (222) at low temperature by rf sputtering, CrystEngComm 12 (2010) 3172–3176.

[15] L. Haifei, X. Xiaoliang, L. Liu, G. Maogang, L.J. Yansong, Photoluminescence enhancement of ZnO microrods coated with Ag nanoparticles, Journal of Physics: Condensed Matter 20 (2008) 472202–472206.

[16] C.A. Lin, D.S. Tsai, C.Y. Chen, J.H. He, Significant enhancement of yellow–green light emission of ZnO nanorodarrays using Ag island films, Nanoscale 3 (2011) 1195–1199.

[17] J.B. You, X.W. Zhang, Y.M. Fan, Z.G. Yin, P.F. Cai, N.F. Chen, Effects of the morphology of ZnO/Ag interface on the surface-plasmon-enhanced emission of ZnO films, Journal of Physics D: Applied Physics 41 (2008) 205101–205105.

[18] Y.C. Liang, C.Y. Hu, H. Zhong, Effects of ultrathin layers on the growth of vertically aligned wurtzite ZnO nanostructures on perovskite single-crystal substrates, Applied Surface Science 261 (2012) 633–639.